

## **A soil-water retention function that includes the nearly dry region through the BET adsorption isotherm**

**Orlando Silva and Jordi Grifoll\***

Grup de recerca de Fenòmens de Transport  
Departament d'Enginyeria Química,  
Universitat Rovira i Virgili,  
Av. dels Països Catalans 26,  
43007 Tarragona, Spain.

\*Corresponding author. Tel.: +34 977 55 96 39; fax +34 977 55 96 21

*E-mail addresses:*

[orlando.silva@urv.cat](mailto:orlando.silva@urv.cat) (O. Silva), [jordi.grifoll@urv.cat](mailto:jordi.grifoll@urv.cat) (J. Grifoll)

### **Abstract**

Most existing full-range soil-water retention functions extend standard capillary pressure curves into the dry region to zero water content at a finite matric potential. A description of dryness is commonly taken as oven-dry conditions given by a matric suction of  $10^7$  cm at zero liquid saturation. However, no finite pressure can be exerted by a zero amount of water, so a more realistic situation necessarily implies that as water content approaches zero, suction tends to infinite. Therefore, the Brunauer-Emmett-Teller (BET) adsorption isotherm arises as a suitable model to describe the water retention in the dry end. In this study we propose a full-range water retention function that takes advantage of the physical consistence of BET adsorption to describe the very dry end, and preserves the capillary behavior of the classical Brooks and Corey function in the wet range. The transition from capillary to adsorption mechanisms is accounted for by a generalization of the Bradley's isotherm. Tests on seven widely studied soil data sets show that the experimental water retention curves are well fitted by the proposed retention model. Finally, the present soil-water retention function was evaluated in a water transport model. In order to test the present approach, our simulations were compared to experimental data for water transport under very dry conditions, found in the literature. The comparison shows that the proposed retention model leads to predictions as good as those resulting from previous full-range soil-water retention functions, while using a physical-based description of the process in the dry region.

## 1. Introduction

Simulation of water flow and chemical transport in the vadose zone requires soil-water retention models. These are mathematical descriptions of the relationship between matric suction and water content. The two most frequently used water retention models have been those proposed by *Brooks and Corey* [1964] (BC) and *van Genuchten* [1980]. Their popularity is due to their ability to fit water retention experimental data in the wet region, where it is often expected that most flow occurs, and owing to the fact that they can also be readily combined with conductivity models [e.g., *Burdine*, 1953; *Mualem*, 1976] in order to yield analytic expressions for relative permeability.

Application of BC and van Genuchten functions is generally unsuitable for the very dry range (matric suctions  $< -150$  m) [*Nimmo*, 1991; *Ross et al.*, 1991]. In fact, one of the disadvantages of the traditional water retention models is that they do not allow water content to be below the "residual water content parameter", an assumption that is physically unrealistic [*Nimmo*, 1991, *Groenevelt and Grant*, 2004]. This may imply little difficulty for some applications, such as wetland studies or humid region agriculture, but others, including water flow and solute transport in arid and semi-arid regions, require a more realistic representation of the hydraulic characteristics over the whole range of saturation. For the fine-textured media the high-suction range can be important even when water content remains high.

Empirical extensions for the dry range have been given by several authors. *Ross et al.* [1991] modified the *Campbell* [1974] soil-water retention model to extend the retention curve to dryness. They compared their model with the original equation of Campbell, which was extrapolated to oven-dry conditions, finding that the new function fitted experimental data better than the original equation. *Campbell et al.* [1993] showed that their simple linear relationship for the water sorption isotherm [*Campbell and Shiozawa*, 1992] fits experimental data as well as the more complex model of *Fink and Jackson* [1973]. *Rossi and Nimmo* [1994] presented a sum and a junction model, both based on a power law function complemented with a logarithmic function in the dry range. The sum model adds these two components, while the junction model matches them. In both models the continuity of the function and its derivative is assured. Good agreement between both models and seven sets of experimental water retention data was obtained. *Fayer and Simmons* [1995] proposed replacing the residual water content in the BC and van Genuchten functions with the simple water adsorption equation given by *Campbell and Shiozawa* [1992]. *Morel-Seytoux and*

*Nimmo* [1999] extended the BC model into the high suction range using the *Rossi and Nimmo* [1994] junction model. *Webb* [2000] presented a method to extend classical retention functions to zero liquid saturation, without the need to refit the experimental data as in other approaches [*Rossi and Nimmo*, 1994]. *Groenevelt and Grant* [2004] proposed a model that covers the complete retention curve, expressed in terms of the pF scale previously introduced by *Schofield* [1935]. These authors fitted their model to a variety of soils, finding good agreement between experimental data and their soil-water retention function over the whole range of saturation. As *Rossi and Nimmo* [1994] have pointed out, one of the advantages in having a full-range model of water retention is that it can reliably extrapolate the water retention curve beyond the driest measured point, which can help save measurement time at high suctions. However, although these new whole range approaches give a more accurate representation in the dry end, they have the disadvantage of allowing water content to be zero at finite suction [*Rossi and Nimmo*, 1994; *Morel-Seytoux and Nimmo*, 1999; *Groenevelt and Grant*, 2004]. For laboratory conditions (e.g., oven drying at 105°-110 °C in a room at 50% relative humidity), zero water content is defined as oven dryness, which corresponds to a finite suction, generally taken as 10<sup>7</sup> cm (~10<sup>9</sup> Pa). Physically, no finite pressure can be exerted by a zero amount of water, so a more realistic situation necessarily implies that water content will be zero at infinite suction.

In an effort to provide a full-range soil-water retention function that overcomes these difficulties, *Tuller et al.*, [1999] and *Or and Tuller*, [1999] proposed a pore space representation (angular pore space model) that accommodates both capillarity and adsorptive processes on internal surfaces. This alternative approach enables consideration of individual contributions of capillary and adsorptive components to soil water matric potential through the whole range of saturation, and even satisfies the condition of zero water content at infinite suction. However, its implementation in a numerical transport model is cumbersome and many parameters need to be fitted for a particular soil.

While the new full-range functions provide improved representations of the soil-water retention characteristic, their use and evaluation in numerical transport models has been limited. So far the study of *Andraski and Jacobson* [2000] seems to be the one that has explicitly tested the performance of a full-range water-retention function. These authors altered the UNSAT-H numerical model [*Fayer and Jones*, 1990] to incorporate the *Rossi and Nimmo* [1994] water-retention function. Then they compared field measured and simulated water and heat transport in a layered soil during a period of 3.85 years. Their results showed

that simulations using the Rossi-Nimmo (RN) approach compared favorably with those using the traditional BC model and that RN function can improve the prediction of water potentials in near-surface soils, particularly under dry conditions.

It is well known [Chiou and Shoup, 1985; Chen *et al.*, 2000a and 2000b; Chen and Rolston, 2000] that chemical sorption on nearly dry soils is greatly influenced by relative humidity. Therefore, it is expected that a physically accurate description of the moisture behavior in a very dry soil could also help improve chemical and water transport simulations.

In this paper, a robust and physically meaningful full-range soil-water retention function is proposed. In addition of accommodating the BC functionality in the wet range of the curve, this proposed function is in accordance with the Brunauer-Emmett-Teller (BET) adsorption isotherm in the dry range. A smooth transition from pure adsorption to pure capillarity is accomplished by a generalization of Bradley's isotherm. To assess the accuracy and suitability of the present approach, we have implemented the new water retention function in a water transport model, and have simulated an experiment of continuous evaporation from a soil with low initial water content, comparing with experimental data found in the literature.

## 2. Soil-Water Retention Model

### 2.1. Formulation

We followed a procedure similar to the one described by Rossi and Nimmo [1994] to build up the soil-water retention model. In the wet region, the relationship between the matric pressure  $P$  (Pa) and the volumetric water content  $\theta_w$ , has been taken from the original BC model. Unlike Rossi and Nimmo [1994] who adopted a parabolic correction near saturation, we considered the conventional BC including the air-entry pressure at saturation. We did not alter this part because an air-entry pressure is necessary to describe the capillary fringe, a tension-saturated zone bordering the water table. In fact, there is evidence [Ippisch *et al.*, 2006, Vogel *et al.*, 2000] that inclusion of an air-entry pressure is necessary when using the statistical approaches of Mualem or Burdine to describe the unsaturated conductivity. Ippisch *et al.* [2006] have shown that ignoring the air-entry pressure may lead to a considerable overestimation of the saturated hydraulic conductivity in the case of inverse parameter estimation, or to considerable underestimation of the unsaturated conductivity when it is derived from measured values of volumetric water content.

Whereas in the wet range the soil-water retention curve is the expression of capillary forces, in the dry range, adsorption dominates the relationship between water content and the forces that hold this water in its condensed state. Water adsorption onto soils has been studied by different authors [Puri *et al.*, 1925; Orchiston, 1952; Chiou and Shoup, 1985; Valsaraj and Thibodeaux, 1988; Rhue *et al.*, 1989; Pennell *et al.*, 1992; Amali *et al.*, 1994; Ruiz *et al.*, 1998; Chen *et al.*, 2000; de Seze *et al.*, 2000] and it has been shown that it can be described by the conventional BET isotherm [Valsaraj, 1995]. This adsorption isotherm is written here as

$$\frac{\theta_w}{\theta_{wm}} = \frac{Bx}{(1-x)[1+(B-1)x]} \quad (1)$$

where

$$\theta_{wm} = W_m (1-\varepsilon) \rho_s / \rho_w \quad (2)$$

is a pseudo-volumetric water content at monolayer capacity and  $\theta_w$  is the volumetric water content of the soil. Also in (2),  $\rho_s$  (kg/m<sup>3</sup>) is the density of the solid-soil phase,  $\rho_w$  (kg/m<sup>3</sup>) is the density of the water, and  $\varepsilon$  (m<sup>3</sup>/m<sup>3</sup>) is the porosity. The mass monolayer capacity  $W_m$  (kg/kg) and  $B$  are characteristic BET isotherm parameters and  $x$  is the relative humidity of the air-soil. The relative humidity is related to the matric pressure according Kelvin's equation [e.g. Bear and Batchmat, 1991]

$$x = \exp\left(\frac{P \hat{V}_w}{R T}\right) \quad (3)$$

where  $P$  (Pa) is the matric pressure,  $\hat{V}_w$  (m<sup>3</sup>/mol) is the liquid molar volume of water,  $R$  is the universal gas constant (Pa m<sup>3</sup>/K mol) and  $T$  (K) is the temperature.

Matric pressure was defined originally to be applied under the action of capillary forces and not under adsorptive forces. Nevertheless, as Baggio *et al.* [1997] suggested, matric pressure definition can be extended to include adsorption considering

$$P = -\frac{\Delta h}{\hat{V}_w} \quad (4)$$

where  $\Delta h$  (J/mol) is the enthalpy difference between water vapor in the gas-phase and the condensed or adsorbed liquid-phase, excluding the latent enthalpy of vaporization. Adopting this definition, matric pressure and Kelvin's equation can be applied in soil-water retention curves in the range of low water contents [Gawin *et al.*, 2002; Schrefler, 2004]. Also noteworthy here is the pF scale introduced by Schofield [1935], which being defined as the logarithm of the height of the water column needed to give the suction in question, is really the logarithm of a free energy difference measured on a gravity scale. As stated by Schofield, "the great virtue of energy relationships is that they hold irrespective of particular mechanisms". As clearly explained by Groenevelt and Grant [2004], because Schofield defined the pF as the logarithm of Buckingham's potential, he meant the pressure component of the Gibbs free energy.

Our proposal is to use equations (1) and (3) as the part of the soil-water retention curve applicable in the "dry" region. Using this approach, water adsorption onto soils and soil-water characteristic curves at low moisture content will be described by the same mechanism and formulation.

Altogether, there are four different regions to be considered along the full range of the retention curve: (i) saturation when matric pressure is higher than air-entry pressure

$$\theta_w = \varepsilon, \quad P \geq P_b \quad (5)$$

(ii) a power law relationship, as proposed by Brooks and Corey [1964], at high water contents where the capillary retention mechanism is dominant

$$\frac{\theta_w - \theta_r}{\varepsilon - \theta_r} = \left( \frac{P}{P_b} \right)^{-\lambda}; \quad P_1 \leq P \leq P_b \quad (6)$$

(iii) a logarithmic behavior at low and medium water contents where multilayer adsorption progressively dominates capillary forces

$$\ln(-P) = a + b\theta_w + c\theta_w^2 + d\theta_w^3; \quad P_2 \leq P \leq P_1 \quad (7)$$

and (iv) a final adsorption region described by the BET isotherm as given in equations (1)-(3) for  $P < P_2$ .

When  $c$  and  $d$  are zero, equation (7) reduces to the Bradley's adsorption isotherm [Bradley, 1936], which has been demonstrated to be in good agreement with experimental data [e.g. Orchiston, 1952]. Indeed, the extension of this equation to dryness was the basic assumption used by Rossi and Nimmo [1994] to develop their model.

To apply the present model for a given soil, the BET isotherm parameters ( $W_m, B$ ) and the Brooks and Corey parameters ( $P_b, \theta_r, \lambda, \varepsilon$ ) must be known or fitted. Available experimental data of water adsorption on various soils [e.g., Orchiston, 1952; Amali *et al.* 1994; de Seze *et al.*, 2000] shows that BET equation (1) gives a good representation up to  $x = 0.3$ . On the other hand, it is well known that the classic models of water retention work well in the plant-available range of soil water, i.e. from saturation to the wilting point (15000 mbar). Therefore, as a general rule, we have assumed that equation (7) for intermediate behavior is valid between the junction pressure  $P_2 \approx -162$  MPa (at 20 °C), corresponding to a relative humidity of  $x_2 = 0.3$ , and the junction pressure  $P_1 = -15000$  mbar, corresponding to the wilting point. Thus, the remaining unknown parameters ( $a, b, c, d$ ) can be calculated from the conditions that ensure continuity of  $\theta_w$  and its first derivative at  $P_1$  between (6) and (7), and at  $P_2$  between (7) and (1). Designating by  $\theta_{w1}$  and  $\theta_{w2}$  the volumetric water content at each matching point, these continuity equations are expressed as

$$a + \theta_{w1}b + \theta_{w1}^2c + \theta_{w1}^3d = \ln(-P_1) \quad (8a)$$

$$b + 2\theta_{w1}c + 3\theta_{w1}^2d = -\frac{1}{\lambda(\theta_{w1} - \theta_r)} \quad (8b)$$

$$a + \theta_{w2}b + \theta_{w2}^2c + \theta_{w2}^3d = \ln(-P_2) \quad (8c)$$

$$b + 2\theta_{w2}c + 3\theta_{w2}^2d = \frac{(1-x_2)^2 [1 + (B-1)x_2]^2}{\theta_{wm} B x_2 \ln(x_2) [1 + (B-1)x_2^2]} \quad (8d)$$

A list of experimental water adsorption BET parameters in soils taken from the literature is given in Table 1. It is apparent that these parameters are soil dependent, with a range of values given by  $0.04 \text{ mg/g} \leq W_m \leq 39.8 \text{ mg/g}$  and  $5 \leq B \leq 128.07$ . In the absence of experimental data, one could take as a first estimate the average of the values listed in

Table 1, which are  $W_m = 13.4$  mg/g and  $B = 23.8$ . The parameters  $\lambda$ ,  $\theta$ ,  $\varepsilon$  and  $P_b$  of the BC retention curve are also soil dependent. Fortunately, there are procedures for estimating these parameters from other, more easily measurable soil properties. For instance, *Rawls and Brakensiek* [1989] gave the average BC parameter values for the different soil textural classes in addition to correlations for estimating these BC parameters from porosity and the clay and sand percentages.

However, when experimental data is available, the normal procedure we propose consists of two steps. First, one has to fit the BET adsorption isotherm (parameters  $W_m$ ,  $B$ ) in the range of relative humidity below  $x_2 = 30\%$ , through the common procedure described by other authors [e.g. *Chen et al.*, 2000a; *de Seze et al.*, 2000]. The second step is to fit the set of parameters ( $\lambda$ ,  $\theta$ ,  $\varepsilon$ ,  $P_b$ ) minimizing the global error of the piecewise soil-water retention function, with the set of parameters ( $a$ ,  $b$ ,  $c$ ,  $d$ ) determined by solving the linear system of equations (8). The nonlinear least squares analysis is a suitable method to follow here. In the majority of cases, porosity is a measured parameter, which reduces to three the number of BC parameters to be fitted. The present piecewise water retention curve was fitted to six data sets from *Campell and Shiozawa* [1992] and one data set from *Schofield* [1935]. The same data sets were used by *Rossi and Nimmo* [1994] and *Morel-Seytoux and Nimmo* [1999] to check their models. Figure 1(a)-(g) shows good agreement between the present soil-water retention curve and the corresponding soil experimental data set. To fit the BC parameters logarithmic transformation was used to provide variance homogeneity. The objective function of this optimization was the square of the root mean square error (RMSE)

$$\text{RMSE} = \sqrt{\frac{1}{N} \sum_{i=1}^N (\log M_i - \log P_i)^2} \quad (9)$$

where  $M_i$  and  $P_i$  are measured and predicted values of the negative matric pressure, respectively, and  $N$  is the total number of measurements. The fitting parameters for each soil obtained by the strategy described above are given in Table 2. Additionally, we have included in Table 3 the  $R^2$  values for the BET fit, the RMSE (equation (9)), and the maximum and average  $\theta_w$  discrepancies between the present approach and the experimental data, calculated in the range of matric potential lower than -15000 mbar (wilting point). In general, when comparing different full-range soil-water retention functions one can observe that all of them

fit the experimental data reasonably well. Obviously, the majority of the various proposals are similar because each adjusts its own set of parameters in order to minimize the error. The advantages of using a given model lie in its complexity (number of parameters) and whether it needs to refit the experimental data or not [*Webb*, 2000]. A major difference between the present model and the other approaches is the behavior of the curve as  $\theta_w$  tends to zero. Whereas most of the other full-range functions have the limiting suction value of  $10^7$  cm (taken as oven dryness), the present proposal tends to infinite suction in accordance with adsorption theories. It should be noted that this limiting suction value of  $10^7$  cm, taken for *Morel-Seytoux and Nimmo* [1999], can not be regarded as universal, contrary to what *Groenevelt and Grant* [2004] state. For instance, for soil #7 (Rothamsted) of the data set used by *Morel-Seytoux and Nimmo* [1999] they had to change the limiting suction value to  $5 \times 10^7$  cm to conveniently fit the retention curve, and *Chen et al.* [2000] fitted a Bradley's isotherm to their experimental data of adsorption of water on Yolo silt loam soil, at 24.5 °C, obtaining a limiting suction of  $1.7 \times 10^7$  cm. Undoubtedly, for most practical purposes the logarithmic law, expressed in the form of the Bradley's isotherm, represents the state of the soil system in the dry end very well. However, it has the inconvenience of predicting a non-physical situation of finite matric potential at zero water content. It should be borne in mind that this is a "fictitious" zero water content, since it has been defined as the water content present while the relative humidity in the soil is 1%, achieved by setting a given combination of temperature and relative humidity in the laboratory [*Schofield*, 1935; *Groenevelt and Grant*, 2004]. One of the advantages of the present approach is that it overcomes this inconsistency, because in the very dry range the BET adsorption isotherm governs the relationship between matric pressure and water content.

## 2.2. Unsaturated hydraulic conductivity

Several models have been developed to calculate the relative permeability from the soil-water retention curve. BC used the equation of *Burdine* [1953] to calculate relative permeabilities from their proposed water retention curve. In this work, Burdine's equation has also been chosen to calculate relative permeability to be consistent with BC model, which has been adopted for the close-to-saturation part of the curve. Burdine's equation is

$$k_{rw} = S^2 \frac{I(S)}{I(1)} \quad (10)$$

where  $S = \theta_w/\varepsilon$  is saturation and  $I(S) = \int_0^S d\chi/p(\chi)^2$ . Burdine's model considers the porous media as a bundle of capillaries where water moves due to pressure gradients with hydraulic radius depending on capillary pressure and saturation. This type of model can not be applicable to the BET region of the proposed curve where adsorbed water has no mobility as a result of hydrodynamic forces. Thus, the integral in equation (10) yields

$$I(S) = \begin{cases} 0 & S \leq S_2 \\ I_{iii}(S) & S_2 \leq S \leq S_1 \\ I_{iii}(S_1) + \frac{\lambda}{\lambda+2} \frac{(1-S_r)}{P_b^2} (S_e^{1+2/\lambda} - S_{e1}^{1+2/\lambda}) & S_1 \leq S \leq 1 \end{cases} \quad (11)$$

where  $S_e = (S - S_r)/(1 - S_r)$  is the effective liquid saturation, and  $S_k$  ( $k = 1, 2$ ) is saturation at the junction points  $P_k$  and

$$I_{iii}(S) = e^{-2a} \int_0^S \exp[-2\varepsilon(b\chi + c\varepsilon\chi^2 + d\varepsilon^2\chi^3)] d\chi \quad (12)$$

represents the Burdine's integral function in the region of logarithmic behavior (equation (7)) and it has to be calculated numerically.

### 3. Testing the soil-water retention function in a water transport model

In order to test the accuracy of present approach, we have incorporated the new soil-water retention function in a water transport numerical simulator. A suitable simulation scenario must involve very low water content conditions, for which BET adsorption mechanism governs the relationship between matric pressure and moisture. The testing exercise is divided into two parts. First, in section 3.1 we present the governing equations used in the numerical model and details of the numerical implementation. Then, in section 3.2 we use the water transport model and our soil-water retention function to simulate one of the

experiments of *Chen et al.* [2000b] for an initial condition of low water content. This experiment involved the continuous evaporation of a soil column under atmospheric conditions of varying relative humidity. Therefore, at least close to the soil surface where evaporation occurs, the soil was expected to reach conditions of very low liquid content ( $\theta_w < 0.10$ ), for which soil-water retention will be dominated by the BET branch of the present approach (equation (1)).

#### 3.1. Governing Equations and numerical implementation

The unsaturated soil system considered consists of liquid ( $l$ ), gas ( $g$ ) and solid ( $s$ ) phases. When deriving the transport model equations, we assume that (i) the soil system is under isothermal conditions, (ii) the water is in equilibrium in all phases at all times, (iii) the advection in the gas-phase is negligible and (iv) spatial variations are only considered in  $z$  direction (depth). The mass-conservation equation for water can be described by [*Silva and Grifoll, 2007*]

$$\frac{\partial}{\partial t} (\theta_w \rho_w + \theta_g \rho_v) = -\frac{\partial}{\partial z} (\rho_w q_l + J_{Wg}) \quad (13)$$

where  $\rho_w$  ( $\text{kg/m}^3$ ) is the liquid water density,  $\theta_i$  ( $\text{m}^3/\text{m}^3$ ) is the volumetric fraction of phase  $i$  ( $i = w, g$ ),  $\rho_v$  ( $\text{kg/m}^3$ ) is the water vapor density, and  $q_l$  ( $\text{m/s}$ ) is the specific discharge of the liquid-phase, which is given by the generalized Darcy's law [*Bear and Bachmat, 1991*]

$$q_l = -\frac{k k_{rw}}{\mu_w} \left( \frac{\partial P}{\partial z} - \rho_w g \right) \quad (14)$$

In equation (14),  $k$  is the intrinsic permeability of the soil ( $\text{m}^2$ ),  $g$  ( $\text{m/s}^2$ ) is the gravity acceleration,  $k_{rw}$  is the relative permeability (dimensionless) and  $\mu_w$  ( $\text{kg/m-s}$ ) is the dynamic viscosity of water. The diffusive mass flux of water vapor,  $J_{Wg}$ , is expressed as [*Bear and Bachmat, 1991*]

$$J_{Wg} = -\theta_g D_{Wg} \frac{\partial \rho_v}{\partial z} \quad (15)$$

where  $D_{Wg}$  ( $m^2/s$ ) is the effective water vapor diffusion coefficient in the air within the porous medium. The water vapor density was calculated assuming ideal gas behavior and correcting for the curvature effect of the gas-liquid interface, as stated by Kelvin's equation [Bear and Bachmat, 1991]

$$\rho_v = \frac{p^* M_w}{R T} \quad (16)$$

where  $p^*$  (Pa) is the vapor pressure at the working temperature  $T$  (K),  $M_w = 0.018016$  kg/mol is the water molecular mass and  $R = 8.314$  Pa  $m^3/K$  mol is the universal gas constant.

A dynamic boundary condition at the surface was set to accommodate the evaporation flux,  $N_{Wo}$  ( $kg/m^2$  s). This flux was calculated by considering a mass transfer limitation from the soil surface to the bulk atmosphere [Brutsaert, 1982]

$$N_{Wo} = k_{Wo}(\rho_{Wbk} - \rho_{vo}) \quad (17)$$

where  $k_{Wo}$  (m/s) denotes the atmosphere-side mass transfer coefficients for water,  $\rho_{Wbk}$  ( $kg/m^3$ ) is the background water vapor density in the atmosphere, while  $\rho_{vo}$  ( $kg/m^3$ ) is the water vapor density at the soil surface. The boundary condition at the bottom was set as zero diffusive flux and zero matric pressure gradient.

The effective diffusion coefficient of the water vapor,  $D_{Wg}$  ( $m^2/s$ ), was calculated as

$$D_{Wg} = \frac{D_{Wog}}{\tau_g} \quad (18)$$

where  $D_{Wog}$  ( $m^2/s$ ) is the molecular diffusion coefficient of water in the gas-phase, and  $\tau_g$  (dimensionless) is the tortuosity of the gas-phase. Tortuosity,  $\tau_g$ , was evaluated according to the first model of Millington and Quirk [Jin and Jury, 1996], i.e.  $\tau_g = \varepsilon^{2/3}/\theta_g$ .

The governing partial differential equation for water transport (equation (13)) was discretized spatially and temporally in algebraic form using the finite volumes method with a fully implicit scheme (backward Euler) for time integration [Patankar, 1980]. The non-linear discretized governing equation was solved for the matric pressure using the multivariable

Newton-Raphson iteration technique [Kelley, 1995], with a finite difference approximation of the Jacobian coefficient matrix [Kelley, 1995; Press et al., 1986-1992] and the numerical algorithm described by Silva and Grifoll [2007]. The total soil depth of the simulation domain was set equal to 20 cm. The grid was set uniform with a grid spacing of  $\Delta z = 0.1$  cm, and the time step was allowed to vary without exceeding a maximum time step of 144 s as in Chen et al. [2000b] and Chen and Rolston [2000].

### 3.2. Water Transport Simulation

The water transport model described above and the present soil-water function were used to simulate the LW2 or low initial water content experiment performed by Chen et al. [2000b]. In this experiment, a soil column of about 20 cm length was subject to a continuous evaporation condition at surface. The relative humidity of the sweep gas alternately changed from wet to dry conditions (dry  $N_2$ , with relative humidity 0%; wet air, with relative humidity 97%). The sequence defining the background concentration of water in the sweep gas,  $\rho_{Wbk}$  (equation (17)) was: wet air – dry  $N_2$  – wet air – dry  $N_2$  – wet air. The soil was Yolo silt loam, for which the water adsorption BET parameters are [Chen et al., 2000a]:  $B = 128.07$  and  $W_m = 15$  (mg/g). The adsorption measurements were carried out in the range of relative humidity from about 5% to almost 100%. Also, Chen et al. [2000b] measured the matric pressure at different water contents by a Tempe pressure cell and a pressure plate, and then fitted the data to the Campbell water retention curve [Campbell 1974]. Because the lack of the explicit experimental data in the work of Chen et al. [2000b], we used their fitted retention curve and the experimental adsorption data given by Chen et al. [2000a] to fit our retention function. Additionally, we included the porosity as a fitting parameter, obtaining a value  $\varepsilon = 0.55$ . Note that Chen et al. [2000b] did not explicitly give this parameter, but they indicated that porosity was obtained from soil bulk and particle densities. Assuming a solid particle density equal to  $2.65$  g/cm<sup>3</sup>, and considering that for LW2 experiment the soil bulk density was  $1.27$  g/cm<sup>3</sup>, the estimated porosity would be  $\varepsilon = 0.52$ , a value very close to our fitted porosity. The fitting parameters and the assessment of its accuracy are shown in Tables 2 and 3, respectively. Figure 2 shows the present retention curve fitted by the procedure described in section 2.1 together with the experimental water adsorption data and the Campbell retention curve obtained by Chen et al. [2000b].

Values of  $D_{Wog}$  at 25 °C were taken from Chen et al. [2000b], as  $2.60 \times 10^{-5}$  m<sup>2</sup>/s for water vapor in air, and  $2.64 \times 10^{-5}$  m<sup>2</sup>/s for water vapor in  $N_2$ . For the LW2 experiment, a

measured value of the mass-transfer coefficient of water vapor at soil surface was  $2.36 \times 10^{-3}$  m/s, while the saturated hydraulic conductivity of the soil was  $2.94 \times 10^{-6}$  m/s. The Burdine's integral function in the region of logarithmic behavior (equation (12)) was calculated numerically by an extended trapezoidal rule with a fractional accuracy equal to  $10^{-6}$  [Press *et al.*, 1986-1992]. As described above, the evaporation experiment consisted of five periods: first a wet air period, from 0 to 150.8 h; a first dry  $N_2$  period, from 150.8 to 268.3 h; a second wet air period, from 268.3 to 385.7 h; a second dry  $N_2$  period, from 385.7 to 500 h and a third and last wet air period, from 500 to 623.4 h.

Our simulation results are quite similar to those of *Chen et al.* [2000b]. Figure 3(a) shows that there is good agreement between the measured and simulated evolution of the water mass remaining in the soil. The pattern of weight variation is fairly well predicted by the water transport model using the present retention curve, with a maximum difference of 1.28% between data and simulation results. Figure 3(b) shows the measured and simulated volumetric liquid content profile at the end of the experiment. Both curves are similar, except near the soil top where the predicted volumetric water content is  $0.02 \text{ m}^3/\text{m}^3$  higher than the measured value. It should be taken into account that water content measurements near the soil surface are more difficult owing to the easy development of steep gradients of the different variables in this zone.

The dynamic of the volumetric water content at two depths is shown in Figure 4. The simulated volumetric water contents followed the general trend of measured water content, but did not perfectly matched the experimental data, particularly in the near-surface soil region. Note that TDR measurements give an average value of volumetric water content between the rods. For the measurements at the nominal depth of 1 cm, the two-probe TDR rods were 1 cm apart. Then, assuming a rod diameter of 3 mm ( $\sim 1/8$ "), the water content measured at 1 cm depth will be an average value between 0.35 and 1.65 cm. In Figure 4, the solid lines that represent the calculated water content evolution at 0.35 and 1.65 cm should encompass the reported experimental values at 1 cm of nominal depth. It can be seen that the experimental data is within this band during the wet air periods, but most of the values lie outside it during the dry  $N_2$  periods. At the depth of 10 cm, the volumetric water content was measured by a TDR with rods that were 2 cm apart. Figure 4 shows that these two calculated lines and the experimental data practically coincide during the first wet air and dry  $N_2$  periods. After the first dry  $N_2$  period, the calculated lines start to deviate one from the other, reaching a maximum difference of 8.3% at the end of the simulation. Despite this difference, the

experimental data are encompassed by the two calculated lines representing the nominal depth of the TDR probe. This illustrative figure shows how the mechanism that dominates the water retention at any time and some depths varies during the simulation. For this Yolo silt loam, a water content of  $0.027 \text{ (m}^3/\text{m}^3)$  corresponds to the matching point below which BET adsorption dominates, while between this water content and  $\theta_{w1} = 0.114 \text{ m}^3/\text{m}^3$  (wilting point) the generalized Bradley's isotherm governs water retention. Above  $\theta_{w1}$  there is the capillary region.

Figure 4 shows that during the dry  $N_2$  periods, the simulated water content near the soil surface enters the BET adsorption region, which indicates that this nearly dry region is attainable under natural evaporation conditions. In addition, in the experiments of *Chen et al.* [2000b] they measured the relative humidity at surface and at various depths, and their measurements show that relative humidities at the surface were well below 30% during the dry  $N_2$  periods. This indicates that at least at the surface the water content is governed by adsorption mechanisms that are well described by the proposed water retention curve. Also, it could be expected that these nearly dry conditions are attained in natural arid or semi-arid regions.

Also, from this particular simulation, it can be deduced that, when the present soil-water retention function is used in a water transport model, the predictions are as good as simulation results obtained with other full-range water retention curves, while preserving the description of the adsorption mechanism at low water contents.

In addition, it is well known [*Chiou and Shoup*, 1985; *Chen et al.*, 2000a, 2000b; *Chen and Rolston*, 2000] that chemical sorption on soils is greatly influenced by relative humidity. Therefore, it is expected that a physically accurate description of the moisture behavior in a very dry soil could also help improve chemical transport and volatilization simulations. Transport models of highly sorbing solutes in the vadose zone assume that the solid-gas and solid-liquid equilibrium relationships for chemical are influenced by the fraction of the solid surface area not covered by water molecules. Previous studies have shown that this fraction is best calculated over the full range of water content in terms of the relative humidity and parameter  $B$  of the BET adsorption isotherm, equation (1) [*Hill*, 1946; *Chen et al.*, 2000a].

#### 4. Conclusions



A new full-range soil-water retention function with physical consistence in the dry range has been proposed. The approach takes advantage of the physical consistency and robustness of the BET adsorption isotherm to describe the very dry end, while preserving the capillary behavior of the classical BC function in the wet range. The transition from capillary to adsorption mechanisms is accomplished by a generalization of the Bradley's isotherm, through a relationship between the logarithmic of the matric potential and a cubic polynomial of the water content. Continuity of the function and its derivative is assured through the different regions.

The validity range of the BET adsorption isotherm was established for a relative humidity below 30%. The generalized Bradley's isotherm was used between this point and the wilting point ( $P_1 = -15000$  mbar), above which the classical BC function was chosen because classical models of water retention work well in the plant-available range of soil water.

The proposed water-retention curve is quite similar to other full-range soil-water retention models in most of the saturation range. However, the limiting behavior of matric pressure as dryness is approached is different: while most extended functions predict a finite matric pressure at zero water content, the present proposal predicts an infinite matric pressure according the adsorption theories. Therefore, in simulations using one or the other approaches one could expect differences in situations of low water content. Also, these differences may affect the calculations of organic chemicals transport, since adsorption is highly dependent on relative humidity.

#### Acknowledgments

We gratefully acknowledge the financial assistance received from the DGICYT of Spain, under project FIS2005-07194 and from the Generalitat de Catalunya (2005SGR-00735). We also acknowledge the support received from the DURSI and the European Social Fund.

#### References

- Amali, S., L. W. Petersen, and D. E. Rolston (1994), Modeling multicomponent volatile organic and water vapor adsorption on soils *J. Hazardous Mater.* 36, 89-108.
- Andraski, B. J., and E. A. Jacobson (2000), Testing a full-range soil water retention function in modeling water potential and temperature, *Water Resour. Res.*, 36(10), 3081-3089.
- Baggio, P., C. Bonacina, and B. A. Schrefler (1997), Some considerations on modeling heat and mass transfer in porous media, *Transport Porous Med.* 28, 233-251.
- Bear, J., and Y. Bachmat (1991), *Introduction to modeling of transport phenomena in porous media*. Kluwer academic publishers, Dordrecht.
- Bradley, R. S. (1936), Polymolecular adsorbed films, *J. Chem. Soc.* 139, 1467-1474.
- Brooks, R. H., and A. T. C. Corey (1964), Hydraulic properties of porous media, in *Hydrol. Pap.* 3, Colo. State Univ., Fort Collins.
- Brutsaert, W. (1982), *Evaporation into the atmosphere*, Kluwer academic publishers, Norwell.
- Burdine, N. T. (1953), Relative permeability calculations from pore-size distribution data, *Petroleum Trans.* 198, 71-77.
- Campbell, G. S. (1974), A simple method for determining unsaturated conductivity from moisture retention data, *Soil Sci.* 117, 311-314.
- Campbell, G. S., and S. Shiozawa (1992), Prediction of hydraulic properties of soils using particle size distributions and bulk density data, in *International Workshop on Indirect Methods for Estimating the Hydraulic Properties of Unsaturated Soils*, Univ. of Calif. Press, Berkeley.
- Campbell, G. S., J. D. Jungbauer Jr., S. Shiozawa, and R. D. Hungerford (1993), A one-parameter equation for water sorption isotherms of soils, *Soil Science* 156(5), 302-305.
- Chen D., D. E. Rolston, and T. Yamaguchi (2000a), Calculating partition coefficients of organic vapors in unsaturated soil and clays, *Soil Science* 165(3), 217-225.
- Chen D., D. E. Rolston, and P. Moldrup (2000b), Coupling diazinon volatilization and water evaporation in unsaturated soils: I. Water transport, *Soil Science* 165(9), 681-689.
- Chen D., and D. E. Rolston (2000), Coupling diazinon volatilization and water evaporation in unsaturated soils: II. Diazinon transport, *Soil Science* 165(9), 690-698.
- Chiou, C. T., and T. D. Shoup (1985), Soil sorption of organic vapors and effects of humidity on sorptive mechanism and capacity, *Environ. Sci. Technol.* 19, 1196-1200.

- de Seze, G., K. T. Valsaraj, D. D. Reible, and L. J. Thibodeaux (2000), Sediment-air equilibrium partitioning of semi-volatile hydrophobic organic compounds. Part I. Method development and water vapor sorption isotherm, *Sci. Total Environ.* 253, 15-26.
- Fayer, M. J., and T. L. Jones (1990), UNSAT-H Version 2.0: Unsaturated soil water and heat flow model, *Publ. PNL-6779*, Pac. Northwest Lab., Richland, Wash.
- Fayer, M. J., and C. S. Simmons (1995), Modified soil water retention functions for all matric suctions, *Water Resour. Res.* 31, 1233-1238.
- Fink, D. H., and R. D. Jackson (1973), An equation for describing water vapor adsorption isotherms of soils, *Soil Sci.* 116, 256-261.
- Gawin D, F. Pesavento, and B. A. Schrefler (2002), Modelling of hygro-thermal behaviour and damage of concrete at temperature above the critical point of water, *Int. J. Numer. Anal. Meth. Geomech.* 26, 537-562.
- Groenevelt, P. H., and C. D. Grant (2004), A new model for the soil-water retention curve that solves the problem of residual water contents, *European Journal of Soil Science* 55, 479-485.
- Hill, T. (1946), Theory of multimolecular adsorption from a mixture of gases, *J. Chem. Phys.* 14(4), 268-275.
- Ippisch, O., H.-J. Vogel, and P. Bastian (2006), Validity limits for the van Genuchten-Mualem model and implications for parameter estimation and numerical simulation, *Adv. Water Resour.* 29(12), 1780-1789.
- Jin, Y., and A. Jury (1996), Characterizing the dependence of gas diffusion coefficient on soil properties, *Soil Sci. Soc. Am. J.* 60, 66-71.
- Kelley, C. T. (1995), *Iterative methods for linear and nonlinear equations*, SIAM, Philadelphia.
- Morel-Seytoux, H. J., and J. R. Nimmo (1999), Soil water retention and maximum capillary drive from saturation to oven dryness, *Water Resour. Res.* 35(7), 2031-2041.
- Mualem, Y. (1976), A new model for predicting the hydraulic conductivity of unsaturated porous media, *Water Resour. Res.* 12, 513-522.
- Nimmo, J. R. (1991), Comment on the treatment of residual water content in "A consistent set of parametric models for the two-phase flow of miscible fluid in the Subsurface" by L. Luckner et al., *Water Resour. Res.* 27, 661-662.

- Or, D., and M. Tuller (1999), Liquid retention and interfacial area in variably saturated porous media: Upscaling from single-pore to sample-scale model, *Water Resour. Res.* 35(12), 3591-3605.
- Orchiston, H. D. (1952), Adsorption of water vapor: I. Soils at 25 °C, *Soil Sci.* 76, 453-465.
- Patankar, S. V. (1980), *Numerical heat transfer and fluid flow*, McGraw-Hill, New York.
- Pennell, K. D., R. D. Rhue, P. S. C. Rao, and C. T. Johnston (1992), Vapor-phase sorption of *p*-xylene and water on soils and clay minerals, *Environ. Sci. Technol.* 26, 756-763.
- Press, W. H., S. A. Teukolsky, W. T. Vetterling, and B. P. Flannery (1986-1992), *Numerical recipes in fortran 77: the art of scientific computing*, Cambridge University Press, New York.
- Puri, A. N., E. M. Crowther, and B. A. Keen (1925), The relation between the vapour pressure and water content of soils, *J. Agric. Sci.* 15, 68-88.
- Rawls, W. J., and D. L. Brakensiek (1989), Estimation of soil water retention and hydraulic properties, in *Unsaturated flow in hydrology modeling, theory and practice*, Kluwer Academic Publishers.
- Rhue, R. D., K. D. Pennell, P. S. C. Rao, and W. H. Reve (1989), Competitive adsorption of alkylbenzene and water vapors on predominantly mineral surfaces, *Chemosphere* 18(9-10), 1971-1986.
- Ross, P. J., J. Williams, and K. L. Bristow (1991), Equation for extending water-retention curves to dryness, *Soil Sci. Soc. Am. J.* 55, 923-927.
- Rossi, C., and J. R. Nimmo (1994), Modeling of soil water retention from saturation to oven dryness, *Water Resour. Res.* 30, 701-708.
- Ruiz, J., R. Bilbao, and M. B. Murillo (1998), Adsorption of different VOC onto soil minerals from gas phase: influence of mineral, type of VOC, and air humidity, *Environ. Sci. Technol.* 32, 1079-1084.
- Schofield, R. K. (1935), The pF of the water in soil, *Trans. Int. Congr. Soil Sci.* 3<sup>rd</sup>, II 38-48.
- Schrefler, B. A. (2004), Multiphase flow in deforming porous material, *Int. J. Numer. Anal. Meth. Geomech.* 60, 27-50.
- Silva, O. and J. Grifoll (2007), Non-passive transport of volatile organic compounds in the unsaturated zone, *Adv. Water Resour.* 30, 794-807.
- Tuller, M., D. Or, and L. M. Dudley (1999), Adsorption and capillary condensation in porous media: Liquid retention and interfacial configurations in angular pores, *Water Resour. Res.* 35(7), 1949-1964.

Valsaraj, K. T., and L. J. Thibodeaux (1988), Equilibrium adsorption of chemical vapors on surface soils, landfills and landfarms-a review, *J. Hazardous Mater.* 19, 79-99.

Valsaraj, K. T. (1995), Elements of environmental engineering. Thermodynamics and kinetics. Boca Raton: CRC Press Inc..

van Genuchten, M. T. (1980), A closed-form equation for predicting the hydraulic conductivity of unsaturated flow, *Soil Sci. Soc. Am. J.* 44, 892-898.

Vogel, T., M. Th. van Genuchten, and M. Cislserova (2000), Effect of the shape of the soil hydraulic functions near saturation on variably-saturated flow predictions, *Adv. Water. Resour.* 24, 133-144.

Webb, S. W. (2000), A simple extension of two-phase characteristic curves to include the dry region, *Water Resour. Res.* 36(6), 1425-1430.

**Table 1.** BET adsorption isotherm parameters from literature.

Source	Soil type	B	W <sub>m</sub> (mg/g)
Puri et al. [1925]	5 different soils	15	6
id.	5 different soils	30	19
Orchiston [1952]	podzol from Otago	14.4	39.8
id.	red brown loam from North Auckland	15.2	33.3
id.	meadow soil from Great Barrier Island	13.0	37.3
id.	brown granular clay from North Auckland	15.2	29.8
id.	yellow-gray loam from Malborough	13.7	5.9
id.	alluvial from Canterbury	12.5	7.6
id.	peat soil from Canterbury	12.7	60.4
Chitou and Shoup [1985]	woodburn dry soil (silt soil, 21% kaolinite)	37.6	11.7
Valsaraj and Thibodeaux [1988]	montmorillonite (natural unheated)	21	12.56
id.	montmorillonite (preheated, 105 °C)	23.3	11.67
id.	montmorillonite (Mg-saturated, unheated)	28.4	11.67
id.	montmorillonite (H-saturated, unheated)	15.2	11.86
id.	montmorillonite (Na-saturated, unheated)	5.9	9.31
id.	montmorillonite (natural unheated at 35 °C)	19.6	12.07
id.	illite (natural unheated)	12.1	2.37
id.	illite (Ca-saturated, unheated)	9.2	2.67
id.	illite (Na-saturated, unheated)	8.5	2.83
id.	kaolinite (natural unheated)	37.8	0.17
id.	sand (green sand, unheated)	5	1.89
Rhue et al. [1989]	Li-kaolin	52	2.6
Penmel et al. [1992], Rhue et al. [1989]	Na-kaolin (kaolinite)	20	4.2
id.	silica gel	18	33.8
Amali et al. [1994]	Riverbed sand	25.7	2.3
id.	Yolo silt loam	17.6	8.5
Rutz et al. [1998]	sand	7.11	0.524
id.	limestone	36.29	0.0412
id.	clay	16.13	5.28
Chen et al. [2000]	Yolo silt loam	128.07	15
de Seze et al. [2000]	natural montmorillonite	21	13
id.	lake sediment	53	12.4

**Table 2.** Summary of soil fitting parameters.

Soil	B	$W_m$ , mg/g	$P_b$ , Pa	$\lambda$	$\theta_r$	$\epsilon$
<sup>a</sup> Palouse	67.35	10.87	-4056	0.33	0.037	0.44
<sup>a</sup> Palouse B	17.88	26.90	-2335	0.18	0	0.55
<sup>a</sup> Walla Walla	16.50	8.46	-4043	0.35	0.030	0.39
<sup>a</sup> Salkum	285.7	13.11	-8525	0.28	0	0.48
<sup>a</sup> Royal	8.65	4.20	-5264	0.55	0.029	0.35
<sup>a</sup> L-Soil	29.49	3.31	-1128	0.40	0.014	0.18
<sup>b</sup> Rothamsted	1300	19.93	-12886	0.30	0	0.51
<sup>c</sup> Yolo silt loam	128.07	15	-4614	0.27	0	0.55

<sup>a</sup>Campbell and Shiozawa [1992]

<sup>b</sup>Schofield [1935]

<sup>c</sup>Chen *et al.* [2000a, 2000b]

**Table 3.** Goodness of the present soil-water retention function fit.

Soil	$R^2$ BET	RMSE	$(\Delta\theta_w)_{max}$ (v/v)	$\Delta\theta_p$ (v/v)
<sup>a</sup> Palouse	0.993	0.106	0.0233	0.0039
<sup>a</sup> Palouse B	0.991	0.160	0.0112	0.0031
<sup>a</sup> Walla Walla	0.986	0.089	0.0056	0.0015
<sup>a</sup> Salkum	0.996	0.136	0.0071	0.0026
<sup>a</sup> Royal	0.997	0.102	0.0028	0.0008
<sup>a</sup> L-Soil	0.998	0.185	0.0016	0.0007
<sup>b</sup> Rothamsted	0.998	0.153	0.0071	0.0035
<sup>c</sup> Yolo silt loam	0.955	0.007	0.0049	0.0020

<sup>a</sup>Campbell and Shiozawa [1992]

<sup>b</sup>Schofield [1935]

<sup>c</sup>Chen *et al.* [2000a, 2000b]

## Figure captions

**Figure 1.** Data-model comparison for the present soil-water retention function: (a) Palouse, (b) Palouse B, (c) Walla Walla, (d) Salkum, (e) Royal, (f) L-Soil, (g) Rothamsted.

**Figure 2.** Present soil-water retention model fitted to water adsorption data and Campbell model from Chen *et al.* [2000a, 2000b] (Yolo silt loam soil).

**Figure 3.** Comparison of water transport experimental data LW2 [Chen *et al.*, 2000b] and numerical simulation including the present soil-water retention function (a) percentage of initial water remaining in the soil, (b) water content profile at the end of the experiment.

**Figure 4.** Evolution of measured and calculated volumetric water content at different depths during LW2 experiment [Chen *et al.*, 2000b]. Nominal depths for experimental data: ● 1 cm, ○ 10 cm.

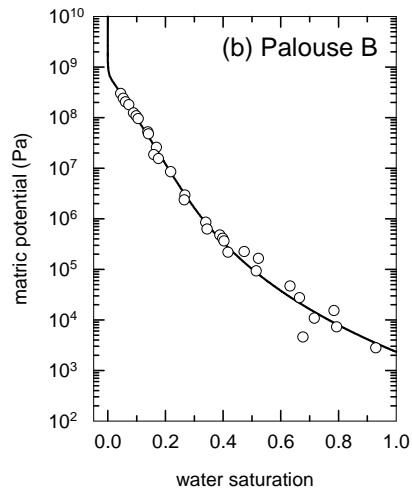
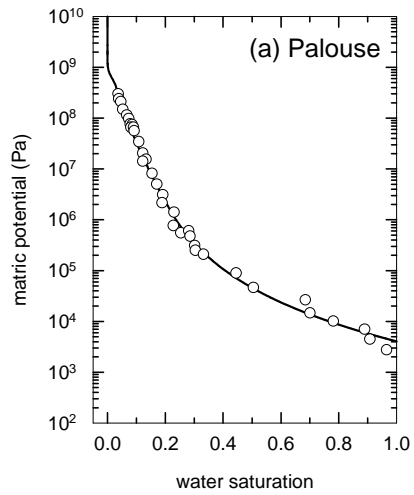


Figure 1(a)-(b)

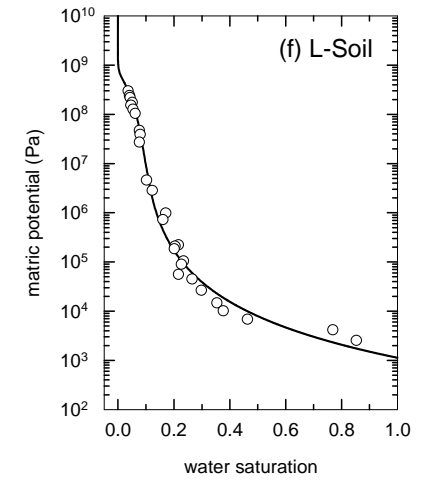
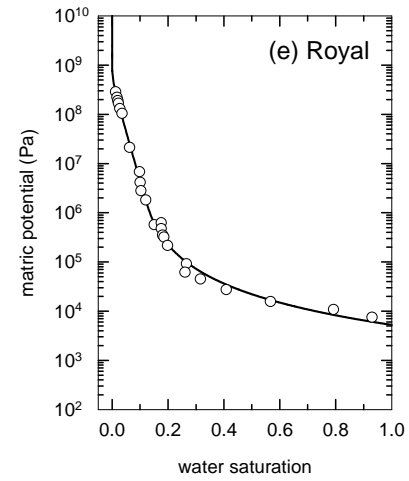


Figure 1(e)-(f)

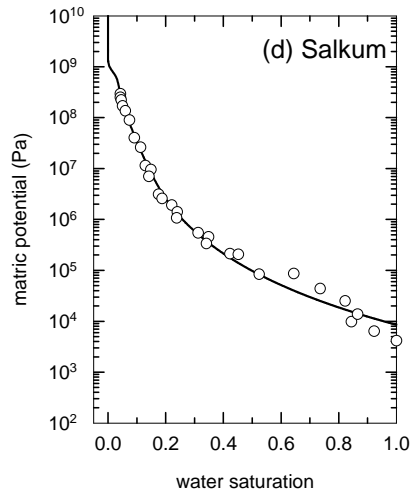
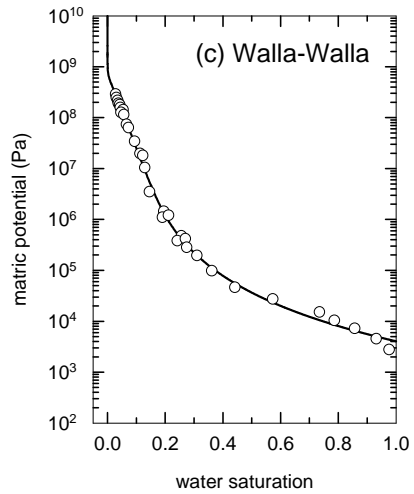


Figure 1(c)-(d)

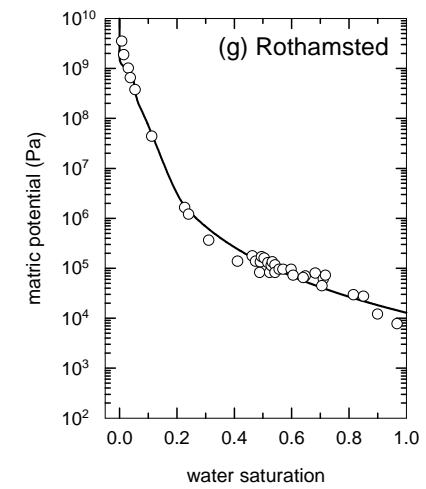


Figure 1(g)

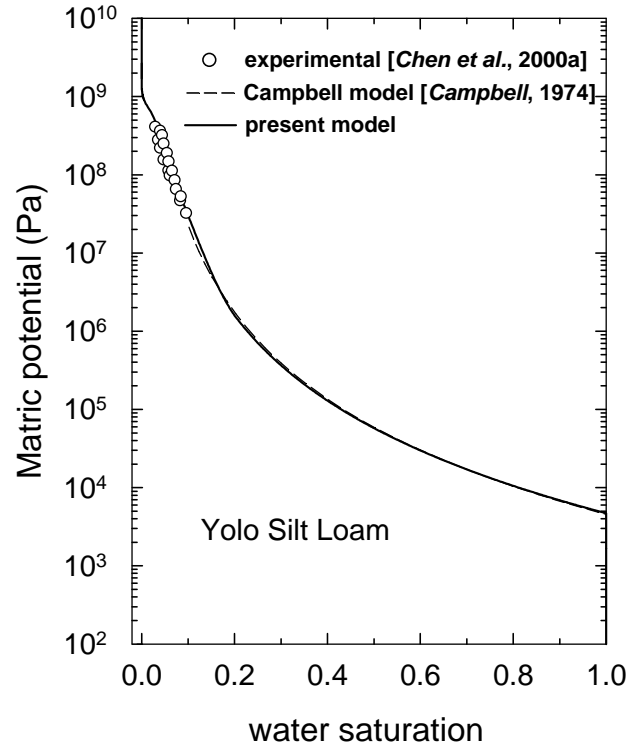


Figure 2

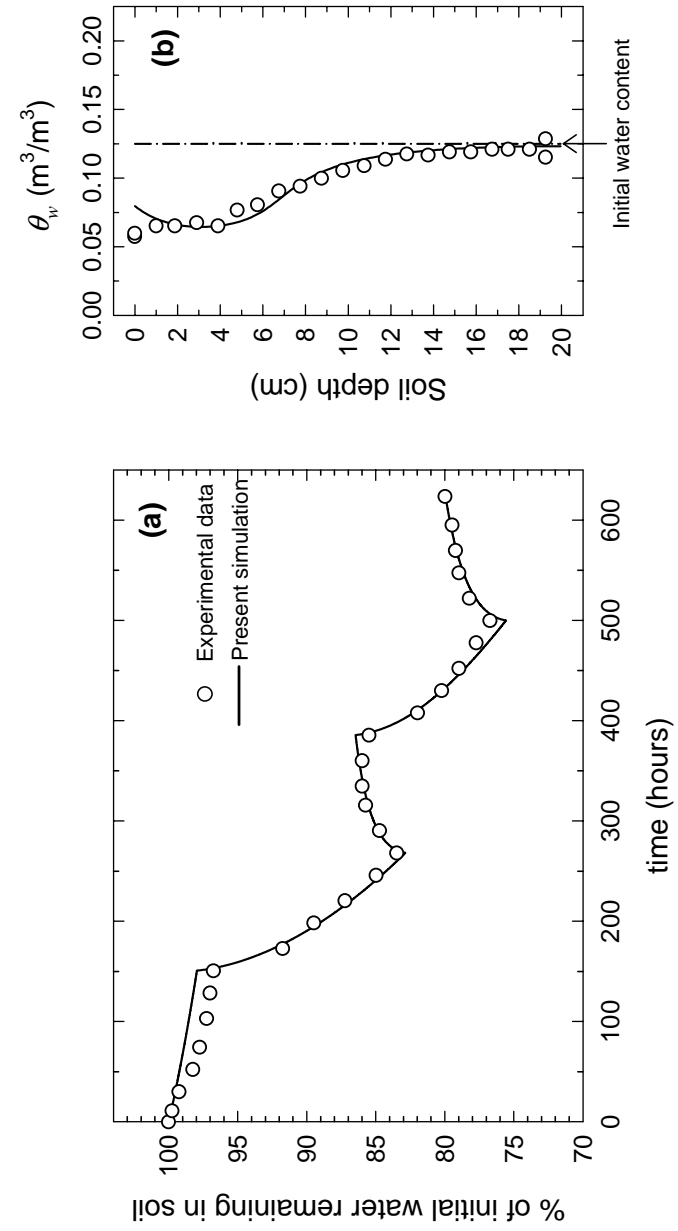


Figure 3

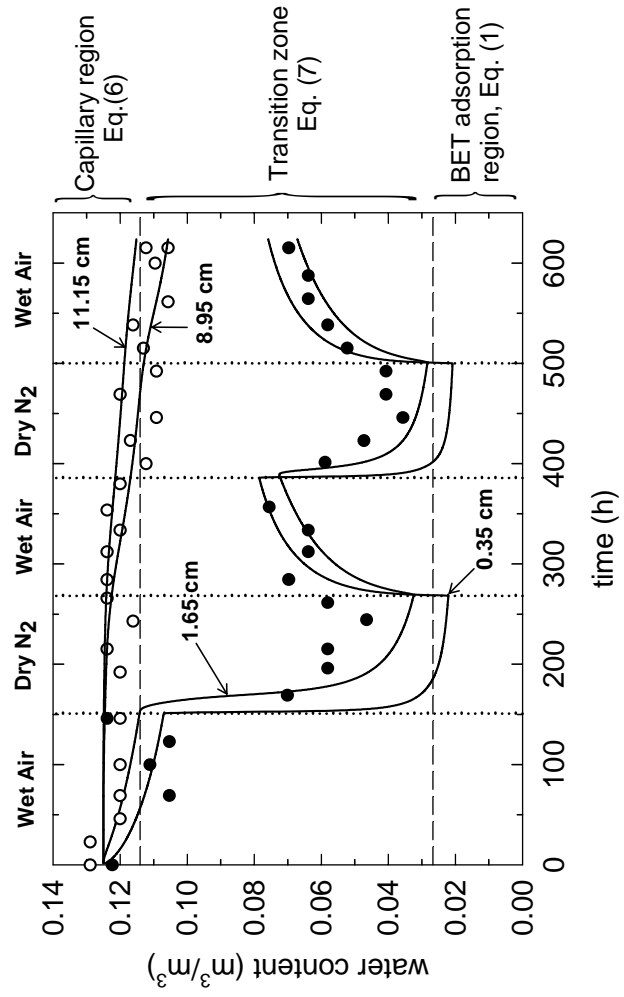


Figure 4